Statistical Properties of Intensity-Based Image Registration Methods

Jeongtae Kim*, *Regular members*

ABSTRACT

We investigated the mean and variance of the MSE and the MI-based image registration methods that have been widely applied for image registration. By using the first order Taylor series expansion, we have approximated the mean and the variance for one-dimensional image registration. The asymptotic results show that the MSE based method is unbiased and efficient for the same image registration problem while the MI-based method shows larger variance. However, for the different modality image registration problem, the MSE based method is largely biased while the MI based method still achieves registration. The results imply that the MI based method achieves robustness to the different image modalities at the cost of inefficiency. The analytical results are supported by simulation results.

Key Words : registration, mean and variance, approximation, mutual information, MSE

Ⅰ. Introduction

Image registration is the task of aligning the same objects in two images. Among many useful applications of image registration, medical image registration is one of the most imporatnt one. For example, since a MRI image provides anatomical information while a PET(Positron Emission Tomography) image does functional information, it can be very useful to view exactly registered two images to view functional information within the anatomical boundary.

The image registration is usually achieved by estimating a geometric transformation that maximizes a *similarity measure* between two images. Therefore, designing a registration method is equivalent to designing a transform estimator. To design an efficient estimator, understanding the statistical properties such as the mean and variance is very important since those properties represent the performance of the estimator.

In general, it is difficult to determine the statistical properties analytically since many estimators are determined implicitly as the maximizers of some objective functions. To overcome the difficulty,, we investigate the mean and variance of an estimator using the first order Taylor series approximation. This approximation was proved to be effective in analyzing the statistical properties of image reconstruction methods [1].

We focus on the MSE (Mean Square Error) based and the MI (Mutual Information) based methods. The MSE based method has been successfully applied for the same modality image registration problem [2] while the MI based method has been effective for the multi-modality image registration problem [3-5].

In this study, our analysis are focused on the same modality problem and simulations are constructed using two 1D signals that are identical except for delay and observation noise. This problem is the same as the delay estimation problem in communications. We have chosen this problem setting not only for the simplicity of analysis but also

* Multimedia Signal processing Lab., Dept. of Information Electronics, Ewha Womans University(jtkim@ewha.ac.kr),
논문번호 : KICS2005-09-366, 접수일자 : 2005년 9월 6일
※ This work was supported by the Ewha Womans University Research Grant of 2004.

for the comparative study since the MSE based method usually do not achieve registration if two images are different.

This paper is organized as follows. In section Ⅱ, we formulate the image registration as a parameter estimator and present the MSE and the MI-based estimator. We present the mean and variance approximation and apply the method for image registration in section Ⅲ. Simulation results are reported in section Ⅳ. Discussions and conclusion are followed in the subsequent sections.

Ⅱ. Theory

2.1 Image Model

We assume that two misregistered images $S=[S_1,\cdots,S_M]$ and $Y=[Y_1,\cdots,Y_M]$ are from the same objects but from different imaging devices as follows:

$$\begin{aligned} S_i &= s_1(\overrightarrow{t_i}) \\ Y_i &= s_2(T_{\bar{\theta}}(\overrightarrow{t_i}))+N_i, \quad i=1,\ldots,M, \end{aligned} \tag{1}$$

where $\overrightarrow{t_i}$ is three dimensional coordinate index, $s_1(\cdot)$ is the given image, $s_2(\cdot)$ is the image of the same object from different imaging device, $T_{\bar{\theta}}$ is a geometrical transformation with parameter $\bar{\theta}$, and N_i is i.i.d Gaussian noise.

For estimating the transform parameter $\bar{\theta}$, we generate an image $X=[X_1,\cdots,X_M]$ by transforming image S_i with parameter θ as follows1):

$$X_i=s_1(T_\theta(\overrightarrow{t_i})), \quad i=1,\ldots,M. \tag{2}$$

Image registration is achieved by determining θ that maximizes a *similarity measure* between $X$and Y. To do that, one must design a similarity measure and a geometric transformation model. Many different geometric transformation models such as rigid, perspective, nonrigid transformations have been studied [7-8]. Also, many different similarity measures such as the MSE and the MI have been investigated [2-3].

As explained in the previous section, for the comparison study, we focus on the 1D delay estimation that is represented as follows:

$$\begin{aligned} Y_i &= s_1(t_i-\bar{\theta})+N_i \\ X_i &= s_1(t_i-\theta), \qquad i=1,\ldots,M. \end{aligned} \tag{3}$$

Using a geometric transformation model and a similarity measure, the estimator is defined as follows:

$$\hat{\theta}=\arg\max_\theta \Phi(X(\theta),Y), \tag{4}$$

where, $\Phi(\cdot,\cdot)$ is a similarity measure, $X(\theta)=[X_1(\theta),\cdots,X_M(\theta)]$.

For 1D delay estimation problem, if the noise is i.i.d. Gaussian, it is known that the MSE can be an effective similarity measure since it yields the MLE (Maximum Likelihood Estimator) [9]. However, if two images are from different modality imaging devices, minimizing MSE does not perform well since MSE can be very large at the registered position. For this multi-modality image registration problem, the MI has been reported to be a very effective similarity measure [3-5].

2.2 MI based Objective Function

The MI between two images X and Y is computed based on the assumption that X_i and Y_i are independent identically distributed samples of two random variables. To compute the MI, we first estimate the joint pdf using the kernel density estimation method as follows [10]:

$$\hat{f}_\theta(x,y;X,Y)=\frac{1}{M}\sum_{i=1}^{M}K(x-X_i(\theta))K(y-Y_i), \tag{5}$$

where, $K(z)=\frac{1}{\sqrt{2\pi\sigma_k^2}}e^{\frac{-z^2}{2\sigma_k^2}}$ with kernel size σ_k^2. We have chosen the kernel density method instead of the histogram method since the kernel based objective function is differentiable2). If the number of samples is infinity, we can acquire an

1) Note that (2) is only conceptual. In practice, since only discrete image is available, interpolation is essential to calculate X_i value from S_i.

insightful formula for the estimated pdf as follows[3]:

$$\lim_{M\to\infty} \widehat{f}_\theta(x, y; X, Y) = \lim_{N\to\infty} \frac{1}{M}\sum_{i=1}^{M} K(x-s_1(\frac{iT_f}{M}-\theta))K(y-s_2(\frac{iT_f}{M}-\tilde{\theta})) = \frac{1}{T_f}\int_0^{T_f} K(x-s_1(t-\theta))K(y-s_2(t-\tilde{\theta}))dt \quad (6)$$

After estimating the joint pdf by the kernel density estimator, we compute the joint entropy with the estimated pdf as follows:

$$\widehat{H}_\theta(X, Y) = -\int_{-\infty}^{+\infty}\int_{-\infty}^{+\infty} \widehat{f}_\theta(x, y; X, Y) \log \widehat{f}_\theta(x, y; X, Y)dxdy. \quad (7)$$

In addition, we can compute the marginal pdf and the marginal entropy as follows:

$$\widehat{f}_\theta(x; X) = \frac{1}{M}\sum_{i=1}^{M} K(x-X_i(\theta)) \quad (8)$$
$$\widehat{H}_\theta(X) = -\int_{\infty}^{\infty} \widehat{f}_\theta(x; X)\log \widehat{f}_\theta(x; X)dx.$$

Finally, the MI is computed using the estimated joint entropies as follows [11]:

$$\widehat{I}_\theta(X, Y) = \widehat{H}_\theta(X) - \widehat{H}_\theta(X, Y). \quad (9)$$

Note that we do not consider the marginal pdf of random variable Y since it is not a function of θ. The MI based method estimates $\tilde{\theta}$ by the maximizer of (19).

The MI is expected to be larger if two images are more registered. This is due to that the joint histogram of the corresponding pixels might be more clustered since the corresponding pixels are from the same parts when two images are registered. Note that the usefulness of the MI for the multi-modality image registration problem can be partly explained by the fact that no assumptions were made on the gray scale of two images.

2) In our analysis, the objective function for an estimator must be differentiable.

3) Without loss of generality, we assume that the sampling interval of images is from 0 to T_f

2.3 *Cramer-Rao* bound for 1D Delay Estimation

The *Cramer-Rao* bound provides useful information about the estimation problem. Since the *Cramer-Rao* bound is the lowest achievable variance bound of any unbiased estimator, if the variance of any unbiased estimator equals the bound, one can consider the estimator efficient.

We compute the *Cramer-Rao* bound of the 1D estimation problem as follows. First, we assume that the noise is i.i.d. Gaussian whose variance is σ_N^2. With the assumption, the pdf of the random vector Y with given $\tilde{\theta}$ is represented as follows [9]:

$$f_Y(y; \tilde{\theta}) = \prod_{i=1}^{M} \frac{1}{\sqrt{2\pi\sigma_N^2}} \exp\frac{-(y_i - s_2(t_i-\tilde{\theta}))^2}{2\sigma_N^2}. \quad (10)$$

Using the pdf, the *Cramer-Rao* bound is computed as follows:

$$-\left\{E\left[\frac{\partial^2 \log f(y; \tilde{\theta})}{\partial^2\tilde{\theta}}\right]\right\}^{-1} = \frac{\sigma_N^2}{\sum_{i=1}^{M}[\frac{ds_2(t_i-\tilde{\theta})}{d\tilde{\theta}}]^2}. \quad (11)$$

Note that as the number of samples goest to infinity, the *Cramer-Rao* bound converges to the following quantity:

$$E[(\hat{\theta}-\tilde{\theta})^2] \ge \frac{\sigma_c^2}{\int_{t_o}^{t_f}[\frac{ds_2(t_i-\tilde{\theta})}{d\tilde{\theta}}]^2}, \quad (12)$$

where σ_c^2 is the value of power spectral density of white Gaussian random process.

Ⅲ. Mean and Variance Approximation

Many estimators are determined implicitly as the maximum of some objective functions. In other words, unknown parameter $\theta = [\theta_1, \ldots, \theta_p]'$ is estimated using observation $Y = [Y_1, \ldots, Y_N]'$ as follows:

$$\hat{\theta} = \arg\max_\theta \Phi(\theta, Y). \quad (13)$$

Since $\hat{\theta} = h(Y) = [h_1(Y) \cdots h_p(Y)]$ is an implicit function of Y, there is generally no analytical expression for the mean and variance of the estimator, thereby making it difficult to study the statistical properties.

For studying the statistical properties of such estimators, an aproximation method using the Taylor series expansion has been proposed and applied successfully [1]. The method approximates the estimator using first order Taylor series around the mean of observation, denoted by $\overline{Y_n}$ as follows:

$$h(Y) \approx h(\overline{Y}) + \sum_n \frac{\partial}{\partial Y_n} h(\overline{Y})(Y_n - \overline{Y_n}). \quad (14)$$

As a result, the mean is approximated as follows:

$$E[\hat{\theta}] = E[h(Y)] \approx h(\overline{Y}). \quad (15)$$

Also, the covariance is approximated as follows:

$$Cov[\hat{\theta}] = Cov[h(Y)] \approx \nabla h(\overline{Y}) Cov[Y][\nabla h(\overline{Y})]'. \quad (16)$$

Above formular (16) is not directly applicable since the analytic expression of $\nabla h(\overline{Y})$ is not available. If the gradient of the objective function equals zero at $h(\overline{Y})$, we can find $\nabla h(\overline{Y})$ using the following equality,

$$0 = \nabla^{20}\Phi(h(\overline{Y}), \overline{Y}) \nabla h(\overline{Y}) + \nabla^{11}\Phi(h(\overline{Y}), \overline{Y}), \quad (17)$$

where the (j,k)th element of the $p \times p$ operator ∇^{20} is $\frac{\partial^2}{\partial\theta_j \partial\theta_k}$, and the (j,n)th element of the $p \times N$ operator ∇^{11} is $\frac{\partial^2}{\partial\theta_j \partial Y_n}$. If we assume that the symmetric matrix $-\nabla^{20}\Phi(h(\overline{Y}), \overline{Y})$ is invertible, we can solve for $\nabla h(\overline{Y})$ as

$$\nabla h(\overline{Y}) = [-\nabla^{20}\Phi(h(\overline{Y}), \overline{Y})]^{-1} \nabla^{11}\Phi(h(\overline{Y}), \overline{Y}). \quad (18)$$

Finally, combining (16) and (18) yields the following covariance approximation:

$$Cov[\hat{\theta}] \approx [-\nabla^{20}\Phi(\overline{\theta}, \overline{Y})]^{-1} \nabla^{11}\Phi(\overline{\theta}, \overline{Y}) Cov[Y] [\nabla^{11}\Phi(\overline{\theta}, \overline{Y})]' [-\nabla^{20}\Phi(\overline{\theta}, \overline{Y})]^{-1}. \quad (19)$$

3.1 Mean and Variance Approximation of the MSE-based Estimator

We approximate the mean and variance of MSE based estimator for the 1D delay estimation problem. As it is well known, the MSE based estimator is the MLE when noise is i.i.d. Gaussian [12]. The MSE based objective function is defined as follows:

$$\Phi(Y, \theta) = L(Y; \theta) = \sum_{i=1}^{N} -(Y_i - s_2(t_i - \theta))^2. \quad (20)$$

Differentiating the objective function with respect to θ yields:

$$\frac{\partial\Phi(Y, \theta)}{\partial\theta} = \sum_{i=1}^{M}(Y_i - s_2(t_i - \theta)) \frac{ds_2(t_i - \theta)}{d\theta}. \quad (21)$$

Evaluating (21) at $\theta = \overline{\theta}$ with $\overline{Y}$ yields:

$$\left.\frac{\partial\Phi(\overline{Y}, \theta)}{\partial\theta}\right|_{\theta=\overline{\theta}} = \sum_{i=1}^{M}(s_2(t_i - \overline{\theta}) - s_2(t_i - \overline{\theta})) \frac{ds_2(t_i - \theta)}{d\theta} = 0. \quad (22)$$

Therefore, $h(\overline{Y}) = \overline{\theta}$, which implies that the mean of the estimator is approximated by $\overline{\theta}$ (i.e., unbiasedness). To approximate the variance, we compute $\frac{\partial^2}{\partial\theta^2}\Phi(\overline{\theta}, \overline{Y}), \frac{\partial^2}{\partial\theta\partial Y_n}\Phi(\overline{\theta}, \overline{Y})$ as follows:

$$\frac{\partial^2}{\partial\theta^2}\Phi(\overline{\theta}, \overline{Y}) = \sum_{i=1}^{M} -[\frac{ds_2(t_i - \overline{\theta})}{d\overline{\theta}}]^2 \quad \frac{\partial^2}{\partial\theta\partial Y_n}\Phi(\overline{\theta}, \overline{Y}) = \frac{ds_2(t_n - \overline{\theta})}{d\overline{\theta}}. \quad (23)$$

As a result, the variance of $\hat{\theta}$ is approximated as follows:

$$Cov[\tilde{\theta}] \approx [-\frac{\partial^2}{\partial\theta^2}\Phi(\tilde{\theta},\overline{Y})]^{-1}\nabla^{11}\Phi(\tilde{\theta},\overline{Y})Cov[Y] \cdot [\nabla^{11}\Phi(\tilde{\theta},\overline{Y})]^T[-\frac{\partial^2}{\partial\theta^2}\Phi(\tilde{\theta},\overline{Y})]^{-1} = \frac{\sigma_N^2}{\sum_{i=1}^{M}\left[\frac{d^2 s_2(t_i-\tilde{\theta})}{d^2\tilde{\theta}}\right]^2} \tag{24}$$

The approximated variance of the MSE based estimator corresponds to the *Cramer-Rao* bound. This result is not surprising since the MLE is asymptotically efficient under some reasonable conditions [13]. However, it is very difficult to desigh the MLE if the image value $s_2(\cdot)$ is not known.

3.2 Mean and Variance Approximation of the MI-based Estimator

We approximate the mean and the variance of the MI based estimator. For the simplicity of approximation, we do not consider the marginal entropy4). In that case, the objective function is equivalent to (7). Differentiating the objective function and evaluating at $\theta=\tilde{\theta}$ yields:

$$\frac{\partial\Phi(\theta,\overline{Y})}{\partial\theta}\bigg|_{\theta=\tilde{\theta}} = \int_{-\infty}^{\infty}\int_{-\infty}^{\infty}\frac{\partial\widehat{f}_{\tilde{\theta}}(x,y;\overline{X},\overline{Y})}{\partial\theta} \log\widehat{f}_{\tilde{\theta}}(x,y,:\overline{XY})dxdy. \tag{25}$$

One can show that the derivative of the estimated pdf equals zero at the true registered position under some reasonable assumptions [14]. This makes sense since each entry of the estimated pdf might reach maximum or minimum when two images are registered. Therefore, (25) equals zero and the estimator is approximated as unbiased estimator.

Based on the similar observations, we approximate $\frac{\partial^2}{\partial\theta^2}\Phi(\overline{\theta},\overline{Y})$ and $\frac{\partial^2}{\partial\theta\partial Y_n}\Phi(\overline{\theta},\overline{Y})$ as follows:

$$\frac{\partial^2}{\partial\theta^2}\Phi(\tilde{\theta},\overline{Y}) \approx \int_{-\infty}^{\infty}\int_{-\infty}^{\infty}\frac{\partial^2\widehat{f}_{\tilde{\theta}}(x,y;\overline{Y})}{\partial\theta^2}\log\widehat{f}_{\tilde{\theta}}(x,y;\overline{Y})dxdy. \tag{26}$$

Moreover, using (6), we further approximate the estimated pdf as follows:

$$\frac{\partial^2}{\partial\theta^2}\widehat{f}_{\tilde{\theta}}(x,y;\overline{Y}) \approx \frac{\partial^2}{\partial\theta^2}\int_0^{T_f}K(x-s(t-\theta))K(y-s(t-\tilde{\theta}))dt\bigg|_{\theta=\tilde{\theta}} \approx \int_0^{T_f}\ddot{K}(x-s(t-\tilde{\theta}))\,\dot{K}(y-s(t-\tilde{\theta}))(\frac{s(t-\tilde{\theta})}{dt})^2dt. \tag{27}$$

Using the similar arguments, we approximate $\frac{\partial^2}{\partial\theta\partial Y_n}\Phi(\overline{\theta},\overline{Y})$ as follows5):

$$\lim_{M\to\infty}\sum_{n=1}^{M}\frac{\partial^2}{\partial\theta\partial Y_n}\mathcal{F}(\tilde{\theta},\overline{Y}) \approx \int_0^{T_f}\dot{K}(x-s(t))\dot{K}(y-s(t))(\frac{s(t)}{dt})^2dt. \tag{28}$$

Finally, using (19), (27), and (28), we approximate the variance as follows:

$$Var[\tilde{\theta}] = \frac{\sigma^2_N}{I_M}, \tag{29}$$

where,

$$I_M = \int_{-\infty}^{\infty}\int_{-\infty}^{\infty}[\int_0^{T_f}\dot{K}(x-s(t))\dot{K}(y-s(t))(\frac{s(t)}{dt})^2dt]\log\widehat{f}_{\tilde{\theta}}(x,y)dxdy$$

Above results also imply that the variance of $\tilde{\theta}$ decreases as the derivative values of images increase. This implies that the high frequency components are helpful for registration, and is consistent with the observations from the *Cramer-Rao* bound. However, the MI-based estimator does not achieve the *Cramer-Rao* low bound as we can understand from the approximation. This result is not surprising since the MI-based estimator did not utilize the information that the two images being registered are the same.

4) For many cases, this assumption is reasonable since the marginal entropy is almost constant even if θ is changed.

5) Without loss of generality, we assume that $\tilde{\theta}=0$.

Ⅳ. Simulation Results

We have implemented numerical simulations for the performance analysis of the MSE-based estimator and the MI-based estimator.

Fig. 1 shows two 1D images that were used for the simulation. The noiseless image was geometrically transformed to achieve registration onto delayed noisy observation. The number of samples was $M = 1000$ and the delay amount was 0.1 pixel.

Fig. 2 and 3 show that the estimated pdfs for registered and mis-registered cases, respectively. One can see that the registered pdf is much more clustered (i.e. larger MI) than mis-registered case. Note that the registered pdf has sharp ridge along diagonal axis since two images are the same except for noise.

We investigated the statistical properties of the estimators empirically using 100 realizations. Fig. 4 and Fig. 5 show the empirical mean and variance of the MSE and the MI based estimator. As expected, both estimators were asymptotically unbiased as shown in Fig. 4. For the variance, the MSE achieved *Cramer-Rao* bound even in the very low SNR region while the performance of the MI based estimator was poorer than the *Cramer-Rao* bound.

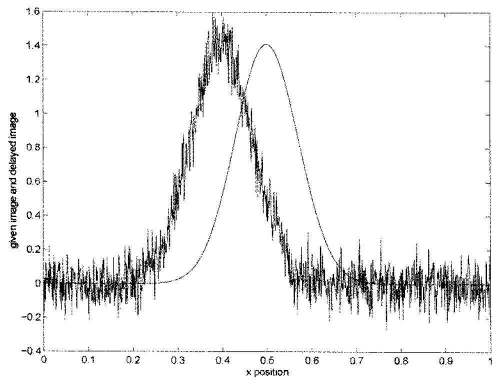

Fig. 1. 1D images.

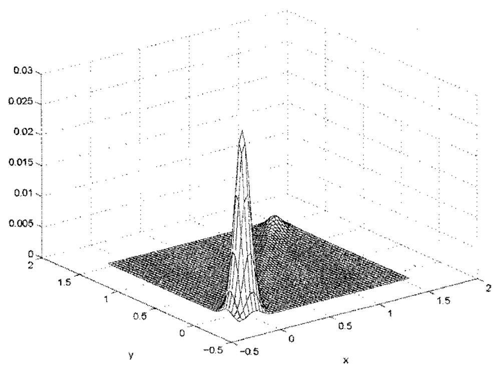

Fig. 2. Registered pdf (kernel size 0.4).

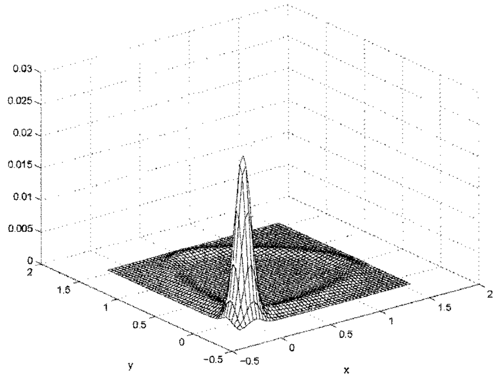

Fig. 3. Misregistered pdf of 0.1 delay (kernel size 0.4).

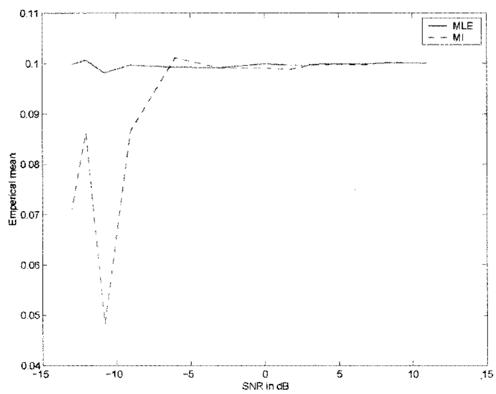

Fig. 4. Emperical mean of estimators vs SNR.

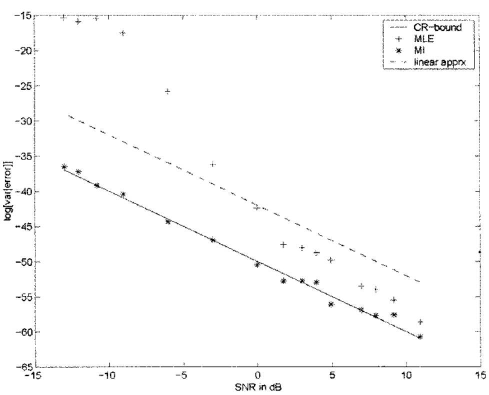

Fig. 5. Empirical variance of estimator vs SNR.

Although the performance of the MI based method was poorer than the MSE based estimator in this experiment, it should be emphasized that the result is when two images are the same. In general, if two images are from different imaging devices, the MSE based method may not achieve registration while the MI based method shows good performance. To investigate those properties, we implemented another simulation using an one-dimensional signal extracted from a 3D CT image. We generated another image using the function $Y=-1.0X+0.7$as in Fig. 6. Since two images are different even when registered, the MSE based method does not achieve registration.

On the contrary, the MI based method performs well as one can see in the shapes of estimated pdfs. Fig. 7 and Fig. 8 show the registered and mis-registered pdf when noisy observation is delayed by 0.1 pixel. Since the registered pdf is much more clustered than the mis-registered one, one can expect good registration result by maximizing the estimated MI.

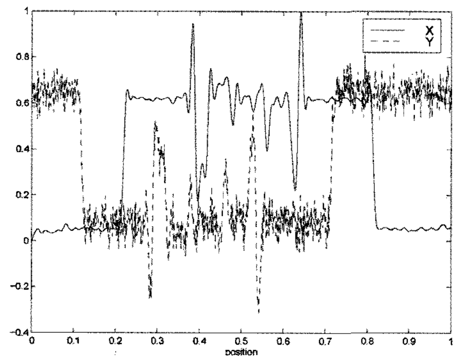

Fig. 6. Multi-modality images.

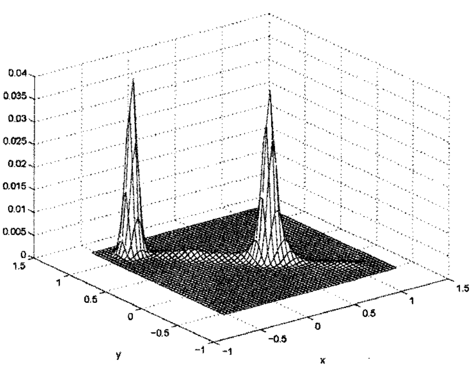

Fig. 7. Registered joint pdf.

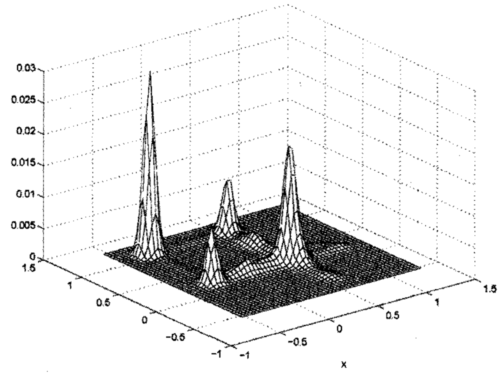

Fig. 8. Mis-registered joint pdf.

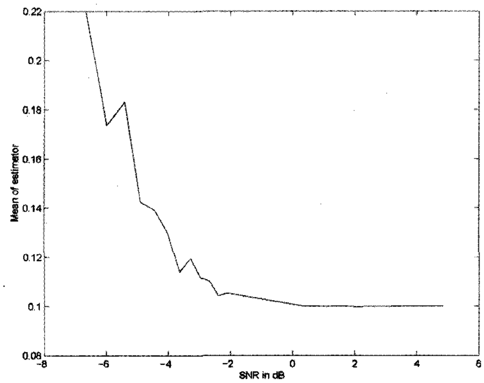

Fig. 9. Mean of the MI based estimator.

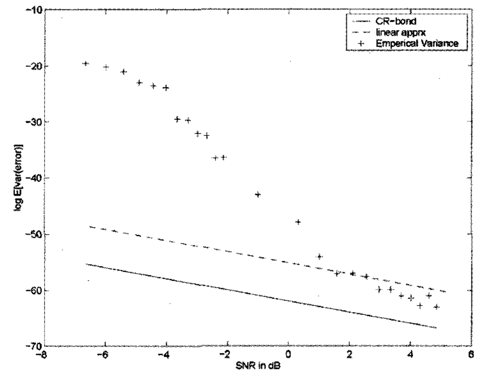

Fig. 10. Variance of the MI based estimator

Fig. 9 and 10 show the empirical mean and the variance of the MI based estimator with *Cramer-Rao* bound. We have not included the result of the MSE-based method since the mean was too much biased (i.e., mis-registered).

As expected, the variance of the MI based method was larger than *Cramer-Rao* bound. One important observation is that the varince and the variance bound were much smaller than that the previous simulation. This fact is due to that the images used in this simulation have much more higher frequency components.

V. Discussion

We have formulated image registration problems as parameter estimator problems and studied the statistical properties of such estimators, especially the MSE and the MI based estimator.

To analyze the statistical properties, we have approximated the estimators using the first order Taylor series expansion. In the asymptotic case of infinite numbers of samples, the MSE based estimator was unbiased and efficient. This result is consistent with the results from Cramer [13] since the MSE based estimator is MLE for the same image registration problem.

The performance of the MI-based method was poorer than the MSE based method since the MI method was not efficient. This result is not surprising since the MI method did not utilize the information that the two images are the same except for noise. However, it should be noted that this phenomenon is true only for highly restricted case of the same image registration.

If two images being registered are different, the MSE based method usually yields large registration error while the MI based method still achieves registration. Even for the same modality image registration, it should be a good idea to use the MI method if two images are not exactly same. For example, there may be objects in only one image. We think that the MI method achieves better *robustness* to *outliers* at the cost of larger variance.

VI. Conclusion

We have analyzed the mean and variance of the MSE based and the MI based image registration methods using the first order Taylor series approximation. The analytical results and simulation results indicate that the MSE based method performs better than MI based method in terms of variance. However, for multi-modality image registration, the MI based method performs better than the MSE based method in terms of bias.

참고문헌

〔1〕 J A Fessler, "Mean and variance of implicitly defined estimators (such as penalized maximum likelihood): Applications to tomography," *IEEE Tr. Im. Proc.*, vol.5, no.3, pp403-506, Mar.1996.

〔2〕 L. Dong and A L boyer, "An image correlation procedure for digitally reconstructed radiographs and electronic portal images," *Int. J. Tadiation Oncology Biol. Phys.*, vol. 33, no. 5, pp. 1053-1060, 1995.

〔3〕 W M Wells, P Viola, H Atsumi, S Nakajima, and R Kikinis, "Multi-modal volume registration by maximization of mutual information," *Med. Im. Anal.*, vol. 1, no.1, pp. 35-51, Mar. 1996.

〔4〕 F Maes, A Collignon, D Vandermulen, and P Sutens, "Multimodality image registration by maximization of mutual information," *IEEE Tr. Med. Im.*, vol. 16, no.2, pp. 187-98, Apr., 1997.

〔5〕 C R Meyer, J L Bose, B Kim, P H Bland *et al.*, "Demonstration of accuracy and clinical versatility of mutual information for automatic multimodality image fusion using affine and thin plate spline warped geometric deformations," *Med. Im. Anal.*, vol. 1no.3, pp. 195-206, 1997.

〔6〕 J Kim and J Fessler, "Intensity-based image registration using robust correlation coefficients," *IEEE Tr. Med. Im.*, vol. 23, no.11, pp.1430-44, Nov. 2004.

〔7〕 J Kybic, P Thvenaz, A Nirkko, and M Unser, "Unwarping of unidirectionally distorted EPI mages," *IEEE Tr. Med. IM.*, vol 19, no. 2, Feb. 2000.

〔8〕 J Kim, J A Fessler, K L Lam, J M Balter and R K TenHaken, "A feasibility study of mutual information based set-up error estimator for radiotherapy," *Medical Physics*, vol.

28, no. 12, pp.2391-2593, 2001.

〔9〕 M D Srinath, P K Rajasekaran, and R Viswanathan, *Introduction to statistical signal processing with applications*. Prentice-Hall, 1996.

〔10〕 B W Silverman, *Nonparametric density estimation*, London:Chapman and Hall, 1987.

〔11〕 T M Cover and J A Thomas, *Elements of information theory*. New York: John Wiley and Sons, 1991.

〔12〕 H L Van Trees, *Detection, estimation and modulation theoyr, Part I*, New York: WIley, 1968.

〔13〕 M Cramer, *Mathematical methods of statistics,* Princeton University Press, 1946.

〔14〕 J Kim, "Intensity-based image registration using robust similarity measure and constrained optimization: Application for radiation therapy," Ph.D dissertation, The University of Michigan, Ann Arbor, 2004.

Jeongtae Kim ***Regular Member***

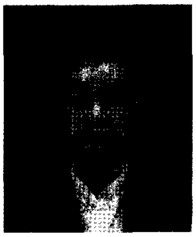

Mar. 1985~Feb. 1989 B. S. from the Dept. of Control and Instrumentation Engineering, Seoul National Univsersity.

Mar. 1989~Feb. 1991 M.S. from the Dept. of Control and Instrumentation Engineering, Seoul National University.

Feb. 1991~Aug. 1998 Senior Resaearch Engineer, Samsung Electronics. Co.

Dec. 2003 Ph.D from the Electrical Engineering and Computer Science The University of Michigan, Ann Arbor, Ph.D.

Mar.2003 Assisstant professor in the Dept. of Information Electronics, Ewha Womans University.